Lithology and Mineral Resources, Vol. 39, No. 3, 2004, pp. 191–202. Translated from Litologiya i Poleznye Iskopaemye, No. 3, 2004, pp. 227–240.

Glauconite at Different Stages of Lithogenesis in Lower Cambrian Rocks of Western Lithuania

T. A. Ivanovskaya and A. R. Geptner

Geological Institute, Russian Academy of Sciences, Pyzhevskii per. 7, Moscow, 119017 Russia
e-mail: remheptner@mtu-net.ru

Received November 5, 2003

Abstract—It is shown that glauconite was mainly formed under diagenetic conditions in terrigenous–clayey rocks (Rausven Unit) of the Lower Cambrian Virbalis Formation in western Lithuania. This was preceded by bioturbation at some levels of geological column and local short-term reworking at other levels. Different forms of glauconite and its interrelation with ambient minerals in diagenesis and epigenesis are considered. A two-phase micaceous (glauconite–illite) composition of globules has been revealed and crystallochemical characteristics of each phase is presented.

Genesis of glauconite in sediments of any lithological type and age remains a debatable issue to date. For example, researchers have proposed different interpretations of the timing of glauconite formation in the multistage process of lithogenesis. Glauconite globules are supposed to be formed during the sedimentation (Formozova, 1949; Hadding, 1932; Lipkina, 1980; Odin, 1975; Shutov *et al.*, 1983; Wilberg, 1980; and others), diagenetic transformation of sediments (Burst, 1958; Geptner and Ivanovskaya, 1998; Hower, 1961; Hohler and Koster, 1976, 1982; Lisitsina *et al.*, 1976; Lisitsina and Butuzova, 1981; Logvinenko *et al.*, 1975; Shutov *et al.*, 1975; Strakhov, 1960; Valeton and Abdul-Razzak, 1975; Valeton *et al.*, 1982; and others), or multistage (sedimentary–diagenetic) processes (Clauer *et al.*, 1992; Fenoshina, 1961; Gorbunova, 1950, 1961; Lazarenko, 1956; Murav'ev, 1983; and others). Discussion of this issue is generally based on the study of authigenic (in situ) glauconite varieties. However, the authigenic reworked and locally redeposited grains can appear in basins with a high hydrodynamic activity. So far, no universal criteria have been elaborated for the classification of authigenic, reworked, and redeposited (terrigenous) grains. Nikolaeva (1977, 1981, 1986) scrutinized this issue and suggested that the main attention should be focused on the comprehensive examination of mineralogical features of different morphological types of glauconite in similar rocks of a single paleobasin.

The lithological, mineralogical, and crystallochemical characteristics of glauconite grains and ambient components and the genesis of this mineral have been discussed in our previous works (Geptner and Ivanovskaya, 1998; 2000; Geptner *et al.*, 1994). In particular, role of the biogenic factor in glauconite formation and issue of the authigenic nature of glauconite globules were discussed in (Geptner and Ivanovskaya, 1998; 2000).

In the present communication, the genesis of glauconite is investigated with Lower Cambrian rocks of Western Lithuania as example. The presence or absence of glauconite grain reworking in the rocks with different structural-textural features (bedding style, bioturbation traces, and so on) and mineral compositions is considered. Possible phases of glauconite formation and transformation at different stages of lithogenesis are discussed. One of the authors (A.R. Geptner) assumes that authigenic glauconite can form as a coating on some glauconite grains at the deep catagenetic stage.

MATERIALS

Glauconite-containing rocks were taken from the Lower Cambrian Virbalis Formation in western Lithuania. The Virbalis Formation (32–40 m) and the underlying Geges Formation (0–30 m) make up the Aischai Group. Based on the presence of acritarchs, rare trilobites, and fragments of brachiopods, chiolites, and others, the Virbalis and Geges formations are considered analogues of the Rausven and Vergal units, respectively (Jankauskas, 2002).

The Virbalis Formation includes an alternation of different proportions of fine-grained sandstones, siltstones, and claystones. The eastern area of Lithuania is dominated by sandstones, whereas the western area is mainly composed of claystones and siltstones.

The rock samples were taken by Ivanovskaya (Geological Institute, Moscow) and Jankauskas (Research Institute of Geological Exploration, Lithuania) in 1989 from boreholes Velaichai-1 and Abling-5 located 30 and 40 km, respectively, from Klaipeda (the distance between the boreholes is 20 km). In Borehole Velaichai-1, the most representative samples were taken from the following intervals, m: 1983–1984 (Sample 89), 1989–1991 (Sample 89/1), 1992–1994

0024-4902/04/3903-0191 © 2004 MAIK "Nauka/Interperiodica"

(Sample 89/4), and 1995–1996 (Sample 89/5). Sample 89/6 was taken at ~2261 m in Borehole Abling-5.

METHODS

Monomineral fractions of glauconite grains were separated by the routine method (crushing, sieving, washing, electromagnetic separation, and final separation under a binocular microscope). Samples 89/4 and 89/6 were divided using heavy liquids into different density fractions ranging from 2.6 to 2.9 g/cm^3 with a spacing of 0.05 g/cm^3.

The glauconite grains were studied by optical, scanning electron microscopic, chemical, X-ray diffraction, and electron diffraction methods with a variable degree of scrutinization. The complete silicate analysis was performed for Sample 89/6 (K.A. Stepanova, analyst). The chemical composition of samples 89, 89/1, and 89/4, including worm-shaped remains, was determined with a Camebax microprobe (G.V. Karpova, analyst). The comparative qualitative analysis was performed using a scanning electron microscope equipped with Link-860 at the Paleontological Institute in Moscow (T.A. Ivanova and L.T. Protasevich, analysts). The X-ray diffraction characteristics were obtained for all samples (E.V. Pokrovskaya, analyst), whereas the electron diffraction characteristics were obtained only for samples 89/4 and 89/6 (S.I. Tsipurskii, analyst).

Macroscopic and microscopic (structural and textural) characteristics of glauconite-containing rocks were studied in polished and thin sections under a binocular microscope. They were scrutinized using a scanning electron microscope equipped with Link-860 at the Paleontological Institute (Moscow). Clay minerals (fractions <1, <2, and <3 μm) and mudstone chips were studied by the X-ray (samples 89/1, 89/4, and 89/6) and electron diffraction (samples 89/4 and 89/6) methods. In addition, minerals extracted from heavy (>2.9 g/cm^3) fractions of samples 89, 89/1, 89/4 (size fraction 0.1–0.05 mm) and Sample 89/6 (0.16–0.1 mm) were examined in the immersion liquid by V.I. Abramenko (Institute of Geology and Geophysics, Belarus).

RESULTS

The studied samples are composed of massive greenish gray sandstones, siltstones and less common dark gray mudstones. Samples of group 1 (89/5 and 89/6) consist of fine-grained sandstones and siltstones with a subordinate clayey material (Figs. 1a–1d). Samples of group 2 (89/1 and 89/4) are composed of siltstones with numerous clayey layers, lenses, and patches (Figs. 1e, 1f). Siltstones of Sample 89 are transitional between groups 1 and 2 in terms of the clayey material content (Figs. 1g, 1h).

Based on structural features, rocks of group 1 (sandstones and siltstones with some clayey material) can be subdivided into horizontal- and oblique-bedded varieties (Figs. 1a–1d). The thickness of layers varies from 1–2 to 10–15 mm. The bedding is emphasized by differences in grain size and/or mineral composition of layers (presence of glauconite, clay minerals, pyritized coatings of organic matter, and so on). Some layers or their patches can be slightly distorted by the sliding and folding of sediments and the activity of mudeaters. The latter feature is typical for horizontal-bedded siltstones with an increased content of clayey material (Figs. 1g, 1h).

In siltstones of group 2 (siltstones with a high content of clayey material), primary sedimentary structures are distorted by the activity of fucoids (Figs. 1e, 1f). Such bioturbation structures (ichnostructures), known as "kraksten," are widespread in Lower Cambrian claystones and siltstones of the Baltic Syneclise (Brangulis *et al.*, 1986, Jankauskas, 2002; Pirrus, 1989 and others).

The sandstones and siltstones are mainly composed of quartz (75–85%), glauconite (10–15%), feldspars (up to 5%), varicolored lamellae (≤3%), as well as fragments of phosphate shells, vermicular remains, and sand-sized phosphate grains.

The matrix composed of clayey, carbonate, and micaceous minerals supplemented with glauconite can be divided into the pore, basal, and pellicular types. If the clayey component is absent, the rock is cemented as a result of the conformation and regeneration of quartz and feldspar grains that are often well crystallized. The coarse-grained dolomite is found as pore and basal matrices. Pyrite occasionally makes up the pore matrix. Pyrite crystals and aggregates are often developed in clayey, organic, and glauconite patches. Titanium minerals (leucoxene and less common anatase) are also widespread in the studied rocks.

Diffraction data show that clayey fractions (<1, <2, and <3 μm) and mudstone chips from glauconite-containing rocks (samples 89, 89/1, 89/4, and 89/60) consists of dioctahedral Fe-illite (b = 9.01–9.03 Å) with an admixture of trioctahedral Fe^{2+}–Mg-chlorite (b = 9.30 Å). Kaolinite is present as traces.

Specific Features of Glauconite Segregations in the Rock

Glauconite is found as globular, anhedral, vermicular, and lamellar grains (Figs. 2a–2f).

The anhedral glauconite is a product of the interaction of globules with ambient terrigenous grains, leading to the formation of convexo-concave globules, splitting of glauconite grains into fragments, or development of pore matrix and specific festoons occasionally connected by thin crosspieces (Figs. 2a, 2b, 2e). In such cases, the glauconite shows a weak pleochroism and wavy (or normal) extinction. The festoons are occasionally characterized by longitudinal jointing.

In clay layers, glauconite grains are found as both globules and lamellae oriented along the bedding. Anhedral, often whimsical glauconite grains are related to the partial replacement by dolomite, quartz, and clayey material.

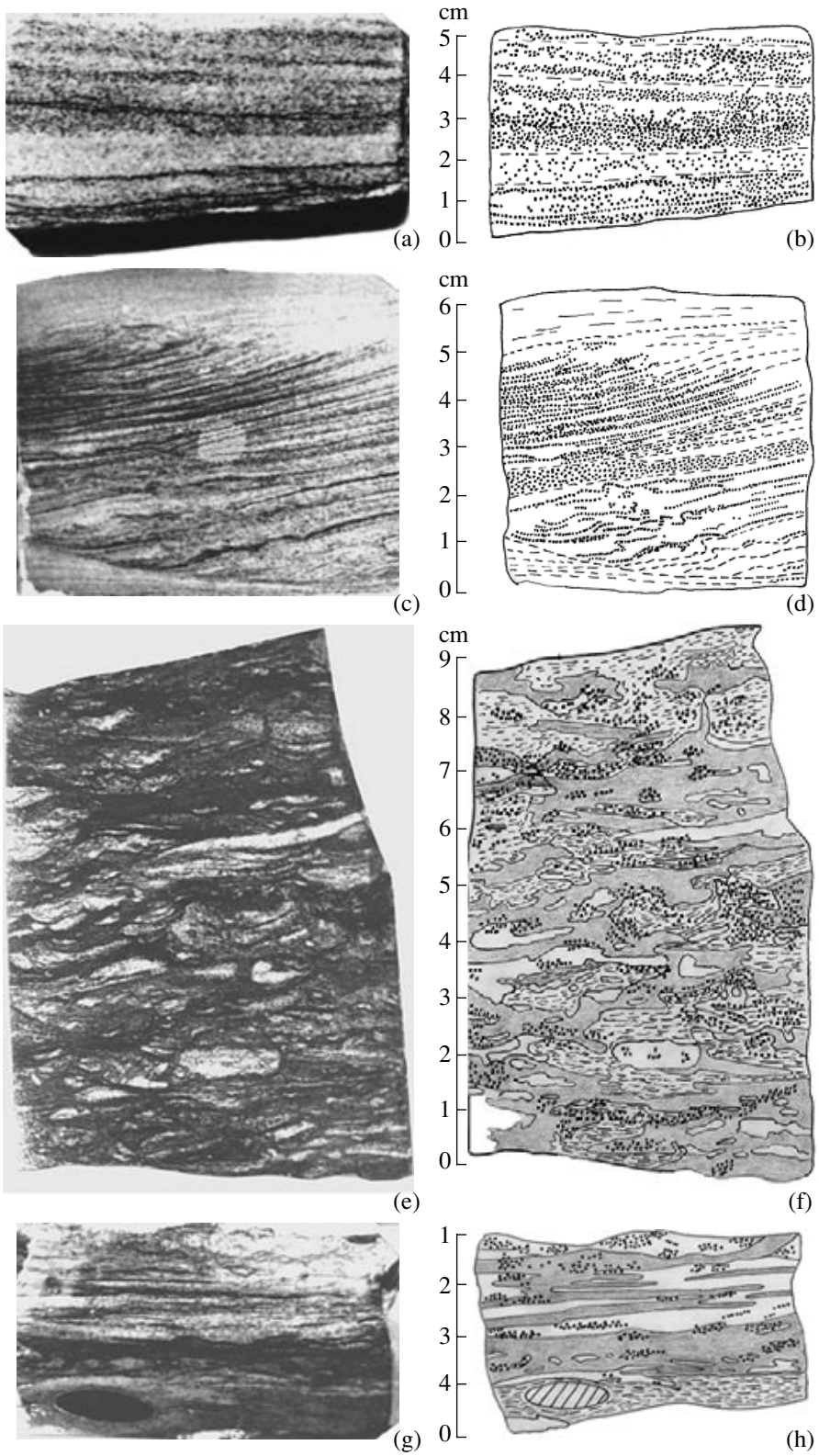

Fig. 1. Photomicrographs (a, c, e, g) and drawings (b, d, f, h) of structural features of glauconite-containing sandstones, siltstones, and claystones. (a, b) Horizontal-bedded structure; (c, d) oblique-bedded structure with traces of creep and folding; (e, f) ichnostructure of the "kraksten" type; (g, h) contact between the ichnostructure (upper part) and the horizontal-bedded rock.

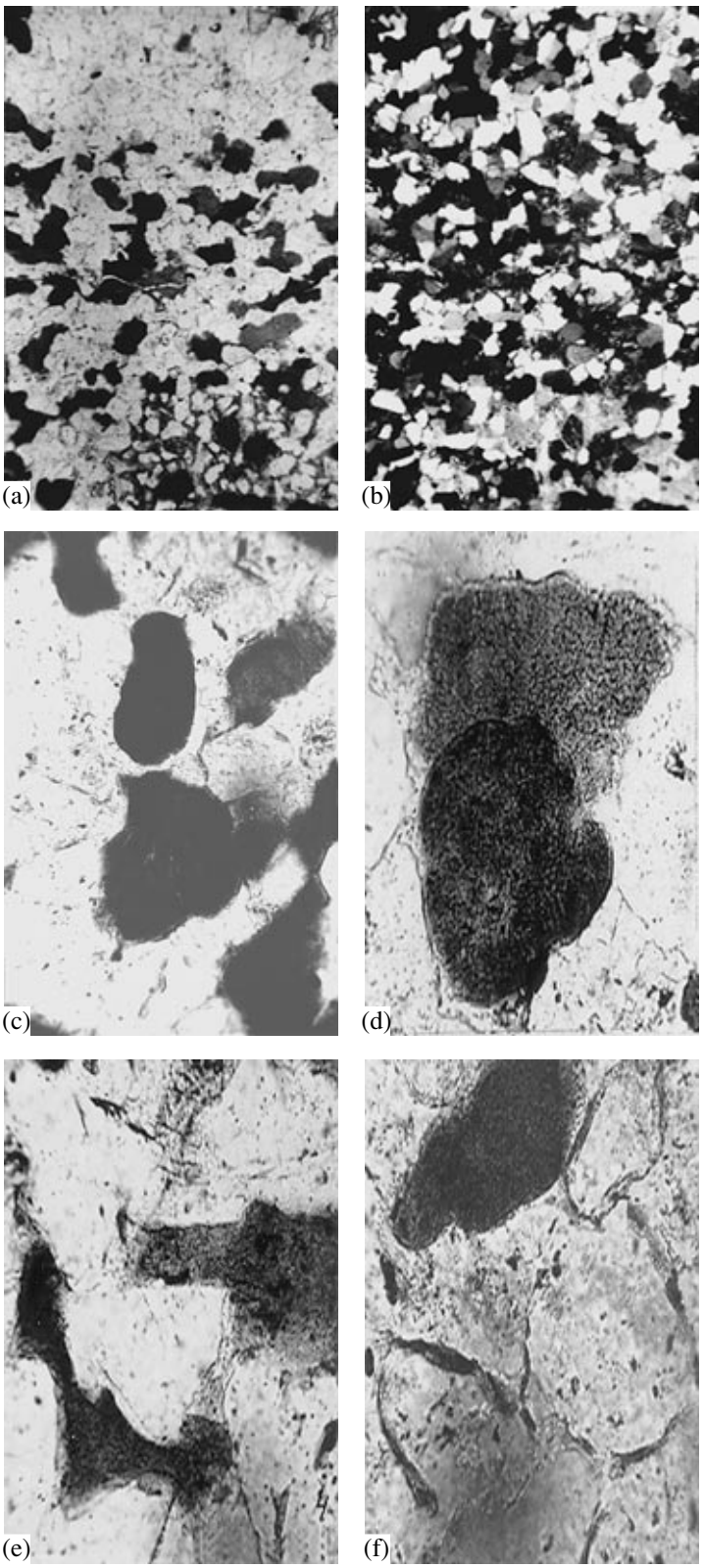

Fig. 2. Interrelation of glauconite and ambient components in silty sandstone composed of glauconite and quartz. (a) Interlayer with abundant glauconite grains (dark), thin section, crossed polars; (b) the same, parallel nicols; (c) glauconite grains with variable morphology; (d) grains with variable porosity; (e) glauconite matrix; (f) glauconite rim on quartz grains. Magnification: (a) 150, (b–f) 300.

Table 1. X-ray characteristics of the studied samples

Sample no.	Grain size, mm	Grain density, g/cm^3	d(001), Å		Expandable layers, %	d(060), Å		Parameter b, Å	
			natural	saturated		illite	glauconite	illite	glauconite
89/6	0.315–0.16	2.65–2.75	10.33	9.94	5–10	1.499	1.511	8.99	9.066
89/4	0.315–0.16	2.65–2.75	10.35	9.94	5–10	1.500	1.511	9.00	9.066
89	0.16–0.1	–	10.52	11.6; 9.83	15–20	1.498	1.509	8.99	9.054
89/1	0.315–0.2	–	10.57	11.0; 9.89	15–20	1.498	1.509	8.99	9.054

Glauconite lamellae make up a series of green to greenish brown and brown varieties. One can also see different colors in single grain. Such grains are optically similar to micas. The lamellae are often deformed and split along edges.

The vermicular shape is typical of green organic remains with pleochroism, normal extinction, and high interference (up to orange-blue). Such grains are 0.16–0.4 mm long and 0.08–0.15 mm thick.

Glauconite is developed as diverse grains, matrix, and fragmentary rims around quartz grains (Fig. 2f). Festoon-shaped rims oriented toward the quartz grain center testify to its replacement by glauconite. The rims are locally sealed by regeneration quartz. Glauconite also fills fractures in quartz and feldspar grains and occasionally corrodes these minerals. Phosphate grains and local zones in phosphate shell fragments may also be replaced by the glauconite.

Thus, interrelation of the glauconite with ambient minerals may be both neutral (without traces of corrosion) and aggressive (corrosion and replacement of quartz, feldspars, and other minerals to a variable extent). In turn, glauconite grains are replaced by pyrite, clay minerals, quartz, and dolomite. In the case of glauconite replacement by quartz, the grain shape can be preserved to a variable extent.

Based on structural features, glauconite grains can be divided into homogeneous and heterogeneous varieties with different values of porosity. Figure 2d demonstrates two types of glauconite grains. The porous grain (upper part of the thin section) has a vague outer boundary that is typical of this mineral.

Grains with homogeneous structure and color are less common than the heterogeneous variety with other mineral inclusions or greenish patches and stringers that differ from the groundmass in terms of texture and extinction mode. The oriented extinction of some glauconite globules may be caused by their interaction with ambient minerals (quartz and dolomite).

The deformed, pyritized, and dolomitized glauconite grains, as well as nearly homogeneous globules, can also be encountered in the lamina within a single thin section.

General Characteristics of Glauconite Grains

We carried out a detailed examination of the globular, anhedral, vermicular and lamellar glauconite grains with uniform, convexo-concave, and corrugated surfaces. The corrugated surface is typical of vermicular remains (Fig. 3c).

The grain size varies from 0.4 to 0.1 mm. Samples 89 and 89/5 are dominated by fine grains (0.16–0.1 mm). Samples 89/1 and 89/4 contain almost equal proportions of fine and coarse grains (0.315–0.16 mm). The coarse fraction prevails in Sample 89/6.

The grain color varies form green (Sample 89/4) to bluish green of various shades (samples 89, 89/1, 89/5, and 89/6). The dependence of color on density is insignificant. The darkest color is typical of the vermicular remains found in the most compact fractions (≥2.75 g/cm^3).

Density characteristics of glauconite grains are rather similar in samples 89/4 and 89/6. Each sample is dominated by the density fraction 2.65–2.75 g/cm^3, whereas the share of light (2.65–2.75 g/cm^3) and heavy (2.75–2.85 g/cm^3) fractions is subordinate.

Diffraction Patterns of Glauconite Grains

The X-ray study of oriented grains showed that the mineral is represented by micaceous (samples 89/4 and 89/6) and hydromiaceous (samples 89 and 89/1) varieties with the expandable layer content of 5–10 and 15–20%, respectively. The hydromicas are characterized by an ordered alternation of mica and smectite layers with a short-range order factor $S > 1$. This is indicated by the presence of two reflections (d = 9.83–9.89 and 11.6–11.0 Å) in diffractograms of ethylene glycol-saturated oriented preparations (Table 1).

Diffractograms of unoriented preparations of all samples are characterized by the presence of two micaceous reflections (d = 1.509–1.511 and 1.498–1.500 Å) in the 060 region (Table 1). This suggests that the studied grains contain two phases of layered silicates. The Fe-phase (glauconite) with b = 9.054–9.066 Å is the major phase, whereas the Al-phase (illite) with b = 8.99–9.00 Å is subordinate. The X-ray powder diffraction patterns, typical of dioctahedral glauconite-series micas, are characterized by package defects related to the rotation of layers by $n = 60°$ (polytype 1Md) (Drits

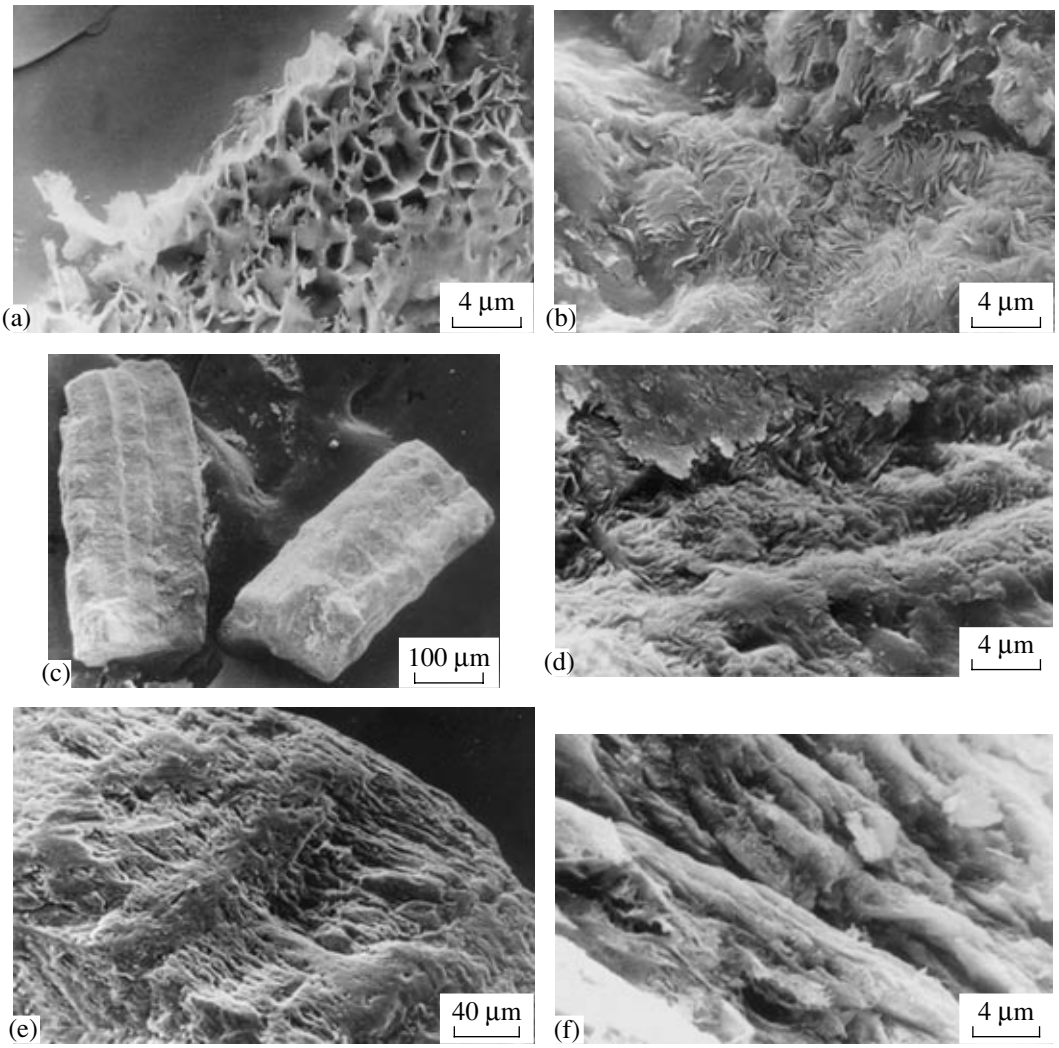

Fig. 3. Microtexture of globular glauconite and vermicular remains replaced by glauconite. Globular glauconite: (a) cellular microtexture, (b) felted microtexture; mineralized biogenic remains: (c) general view from the top showing prominent longitudinal and transverse edges, (d) felted microtexture between transverse edges, (e) microtexture of laminas between transverse edges on the surface of biogenic remains, (f) internal part of biogenic remains showing the microtexture of subparallel-oriented packages.

et al., 1993). The content of defects in the mica structure (parameter P_{ii}) is equal to 0.6–0.65.

Electron diffraction data made it possible to determine elementary parameters of glauconite, parameter *b* of illite (Table 2), and the ratio of these parameters in globules (70 and 30%, respectively).

Chemical Composition of Glauconite Grains

Based on silicate analysis data, Sample 89/6 (size fraction 0.315–0.16 mm, density fraction 2.65–2.75 g/cm^3) has the following composition, %: SiO_2 48.84, Al_2O_3 13.75, Fe_2O_3 16.77, FeO 2.22, MgO 1.94, CaO 0.37, Na_2O 0.26, K_2O 7.23, H_2O^+ 7.21, and H_2O^- 1.79 (total 100.38).

Table 2. Electron diffraction data on the studied samples

Sample no.	Grain size, mm	Grain density, g/cm^3	Parameter of elementary cells				
			illite	glauconite			
			b, Å	*a*, Å	*b*, Å	*c*, Å	β, degrees
89/6	0.315–0.16	2.65–2.75	9.00	5.24	9.07	10.16	101.4
89/4	0.315–0.16	2.65–2.75	8.99	5.24	9.07	10.18	101.2

Table 3. General crystallochemical formula of two-phase globules and compositions and relationships of individual phases (Sample 89/6)

Cations, %	interlayer			octahedral				tetrahedral		b_{exp}, Å	b_{calc}, Å
	K	Na	Ca	Fe^{3+}	Al	Fe^{2+}	Mg	Si	Al		
General composition, 100	0.67	0.04	0.03	0.92	0.74	0.14	0.21	3.56	0.44	–	–
Fe-phase, 70	0.67	0.04	0.03	1.22	0.36	0.20	0.23	3.63	0.37	9.07	9.08
Al-phase, 30	0.67	0.04	0.03	0.20	1.63	–	0.17	3.40	0.6	8.99	8.99

Note: Formulas are based on the anionic composition of $O_{10}(OH)_2$; (exp) experimental; (calc) calculated.

Table 4. Chemical composition of the glauconite-series minerals in globules, wt %

Component	1	2	Average value	3	4	Average value	5	6
SiO_2	49.87	48.96	49.41	50.96	50.86	50.92	51.20	52.46
TiO_2	0.03	0.01	0.02	0.03	0.03	0.03	0.05	0.08
Al_2O_3	15.81	14.63	15.22	14.98	14.39	14.68	11.26	10.72
Fe_2O_3	13.39	14.78	14.08	14.11	15.08	14.60	18.66	19.76
MgO	1.99	2.11	2.05	2.31	2.29	2.30	2.34	2.47
CaO	0.34	0.47	0.41	0.24	0.26	0.25	0.17	0.20
Na_2O	0.02	0.02	0.02	0.03	0.03	0.03	0.01	0.11
K_2O	8.37	8.35	8.36	7.65	7.56	7.61	8.82	8.40
Total	89.82	89.33	89.57	90.31	90.50	90.41	92.00	94.20
Component	Average value	7	8	9	Average value	10	11	Average value
SiO_2	51.83	51.30	49.23	50.50	50.34	50.84	51.56	51.20
TiO_2	0.06	0.04	0.06	0.04	0.05	0.06	0.03	0.05
Al_2O_3	10.99	16.20	13.80	14.45	14.81	14.95	14.37	14.66
Fe_2O_3	19.21	13.61	14.44	14.73	14.26	13.74	14.94	14.34
MgO	2.41	2.58	2.07	2.35	2.33	2.33	2.33	2.33
CaO	0.19	0.26	0.29	0.28	0.27	0.25	0.25	0.25
Na_2O	0.06	0.01	0.05	0.08	0.05	0.06	0.02	0.04
K_2O	8.61	7.69	8.20	8.05	7.98	7.98	8.11	8.05
Total	93.36	91.69	88.14	90.49	90.09	90.21	91.61	90.91

Notes: Analysis nos.: (1, 2): Sample 89/6 (0.315–0.16 mm, 2.65–2.75 g/cm^3), (3, 4) Sample 89/4 (0.315–0.16 mm, 2.65–2.75 g/cm^3), (5, 6) Sample 89/4 (vermicular remains, 0.315–0.16 mm, 2.75–2.8 g/cm^3), (7–9) Sample 89 (0.16–0.1 mm), (10, 11) Sample 89/1 (0.315–0.2 mm). Iron is supposed to be present in the glauconite structure in the three-valent form.

The chemical composition was recalculated to crystallochemical formulas by B.B. Zvyagina using the regressive equation, which correlates parameter *b* of dioctahedral micas with the cation composition (Smolyar and Drits, 1988), and the phase relationship based on electron diffraction data (Table 3). It is evident that the Fe- and Al-phases compositionally fit glauconite and illite, respectively.

Results of the microprobe analysis of globules in samples 89/4 and 89/6 (0.315–0.16 mm, 2.65–2.75 g/cm^3), 89/1 (0.315–0.2 mm), and 89 (0.16–0.1 mm) and vermicular remains in Sample 89/4 (0.4–0.1 mm, 2.75–2.85 g/cm^3) are given in Table 4. The average composition of globules is as follows, %: SiO_2 49.41–51.20, Al_2O_3 14.66–15.22, Fe_2O_3 14.08–14.60, MgO 2.05–2.33, and K_2O 7.61–8.36. Relative to the globular variety, the vermicular glauconite (Sample 89/4) is enriched in Fe and K_2O (Table 4, analysis pairs 3–4 and 5–6, respectively).

The qualitative chemical analysis with scanning electron microscope equipped with Link-860 revealed that green lamellae and globules (Sample 89/6) have similar proportions of major oxides SiO_2, Fe_2O_3, Al_2O_3,

and K_2O, suggesting that the green lamellae compositionally match glauconite.

Thus, relative to the complete silicate analysis, the microprobe data on Sample 89/6 (Table 4, analyses 1, 2) yield underestimated total Fe (~5%) and overestimated K_2O (~1%) contents.

Microtexture of Glauconite Grains

The scanning electron microscope was used to study the following glauconite varieties: (1) fragments of glauconite-containing rocks (samples 89, 89/4, and 89/6); (2) separate glauconite globules (Sample 89/6, 0.315–0.16 mm, 2.65–2.75 g/cm^3); and (3) vermicular remains and green lamellae (Sample 89/6, 0.4–0.16 mm, 2.75–2.85 g/cm^3).

Microtexture of the internal section of globules and vermicular remains can be subdivided into two types (Lisitsina and Butuzova, 1981; Geptner and Ivanovskaya, 1998, 2000; Geptner *et al.*, 1994; Odin, 1975; Odin and Matter, 1981; and others).

Type 1 is developed as cellular microtexture with flakes merging into cells ranging from 0.8 to 4 μm in size (Fig. 3a). Type 2 (felted microtexture) is typical of glauconite (Fig. 3b). It is observed as an aggregate of random, fan-shaped, subparallel, and other forms of differently oriented flakes. The aggregate may be characterized by even or split edges, but the flakes are curved. Both types of internal microtexture are developed within a single globule.

Glauconite lamellae are composed of parallel (or subparallel) and clustered (or isolated) plates. The felted microtexture is occasionally developed in the matrix between the plates.

In terms of microtexture, vermicular remains replaced by glauconite can be similar to the globular glauconite (when both microtextures are present) or the lamellar variety. However, the vermicular variety has some specific features. For example, the mineralized vermicular remains have longitudinal and transverse edges (Fig. 3c). This is clearly seen in the microtextural pattern of glauconite that replaces the vermicular segregation. Against the background of subparallel, differently elongated and curved lamellae, one can see large transverse edges that are often developed on the surface of biogenic remains (Figs. 3d, 3e). Their internal part is composed of poorly crystallized glauconite mass sandwiched between subparallel packages (Fig. 3f).

The globules and vermicular remains are often coated with flakes with even or split edges. The flakes are closely spaced to make up a massive cover (shell) in some areas (Figs. 4a, 4b). Locally, the shell resembles an amorphous mass without any traces of individual flakes (Fig. 4c).

Interrelation of glauconite globules with terrigenous components indicates that some quartz grains are disintegrated (or dissolved) at the contact with glauconite. This is particularly prominent on the glauconite grain surface crumpled by terrigenous particles. At the contact with glauconite, quartz grains have an irregular (often, crenulated) edge. Glauconite flakes penetrate and partly replace the quartz grains along fractures (Fig. 4d).

It is worth mentioning that the contact zone between glauconite and dissolved quartz may be characterized by the typical microtexture of the internal part of globules or the development of the typical shell of globule surface. The shell mimics all irregularities of the glauconite grain surface. At the same time, it is conformable with irregularities on the dissolved quartz grain (Figs. 4e, 4f). On the surface of some glauconite grains with a well-developed shell, one can see numerous holes with crystallographic outlines that are traces of the dissolution of terrigenous components. This is confirmed by the presence of rare terrigenous grains inside the shell (Fig. 4c).

DISCUSSION

The data presented above suggest the following formation and transformation model for the glauconite grains and enclosing rocks at different stages of lithogenesis.

Sedimentary–Diagenetic Stage

As is well known, the formation of glauconite may be a prolonged process often accompanied by turbidity, mixing, and local reworking of sediments. This is evident in sedimentary and postsedimentary structures of glauconite-containing rocks of the Lower Cambrian Virbalis Formation.

Sedimentary structures are observed in clay-poor glauconite-containing quartz sandstones and siltstones as horizontal- and oblique-bedded varieties with some layers slightly distorted by folding, creep, and activity of mudeaters (Figs. 1a–1d). Glauconite grains therein generally follow the bedding pattern, but sometimes they are randomly distributed.

Glauconite grains *in situ* are undoubtedly diagenetic formations in rocks with horizontal bedding typical of calm sedimentation environment (Sample 89/6). Relatively large grains with a narrow density range are widespread in such rocks. Globular varieties are also found (Figs. 2a–2f). The anhedral shape of this mineral is mainly related to the postsedimentary transformation of rocks.

The oblique bedding of rocks (Sample 89/5) is an indicator of the mobile sedimentation environment and, consequently, the possible reworking of glauconite-containing sediments. Glauconite in such rocks is generally fine-grained, whereas larger globular grains are subordinate. Since oblique-bedded rocks are mainly represented by siltstones, glauconite grains are usually larger than the ambient terrigenous components.

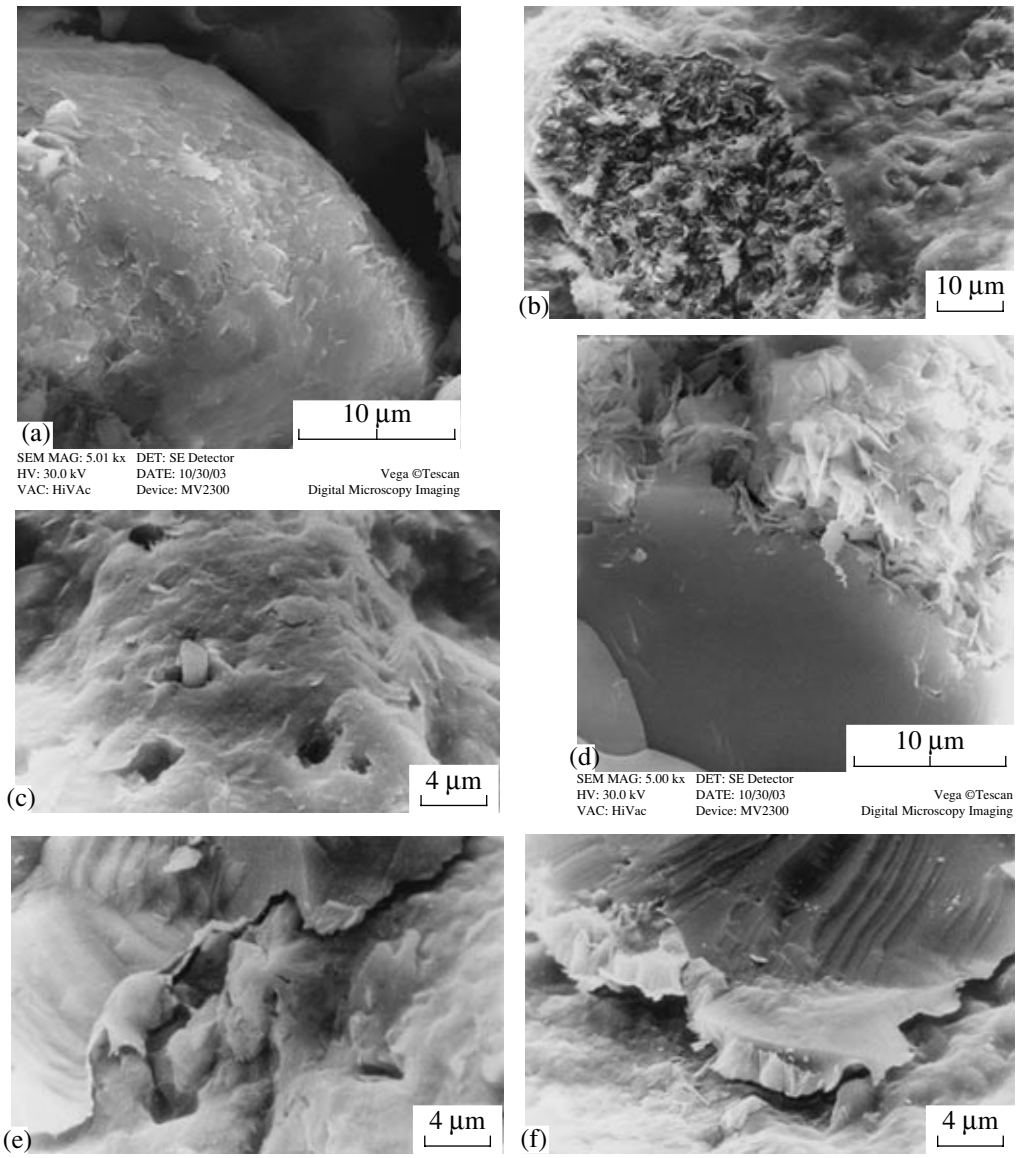

Fig. 4. Microtexture of glauconite shell and interrelation of glauconite globules with terrigenous quartz. Glauconite shell with (a) prominent flakes and (b) numerous holes having crystallographic outlines (traces of dissolved terrigenous components); (c) homogeneous shell with terrigenous grain remains in a hole; (d) uneven contact of quartz grain with glauconite (glauconite flakes intrude and partly replace quartz along cracks); (e, f) shell (conformable with irregularities of the dissolved quartz grain) on glauconite grain surface.

The studied rocks contain both glauconite pseudomorphs (after biotite and vermicular remains) and glauconite grains (similar to their *in situ* counterparts in the overlying units in terms of color, shape, grain size relationship, and other features). This indicates that the glauconite-forming process continued at the diagenetic stage of sediment transformation after short-term reworking episodes.

Postsedimentary structures are related to the distortion of horizontal, lenticular, oblique, and other types of primary bedding of sediments owing to the turbidity, creep, and fucoid activity. As was mentioned above, bioturbation structures are widespread in Lower Cambrian rocks of the Baltic Syneclise. They are also common in Lower Cambrian sections of Lithuania, including the Virbalis section of Borehole Velaichai-1 where one can see postsedimentary structures in sandstones and siltstones with abundant clayey material (Jankauskas, 2002). The initial rocks were probably composed of an alternation of sandy–silty and clayey layers with different thicknesses. The layers are partly disintegrated and whimsically redistributed owing to mixing, roiling, and creep (Figs. 1d, 1f). Moreover, the glauconite clusters are obliquely oriented relative to the bedding, suggesting their formation after the termination of bioturbation, i.e., at the diagenetic stage.

Let us remind that the bioturbation structures are typical of samples 89/1 and 89/4. In terms of morphology, dimension, and density, glauconite grains in Sample 89/4 are similar to authigenic grains in Sample 89/6.

The bioturbation reworking of sediments can be insignificant. For example, synsedimentary (horizontal-bedded) structures are only locally distorted by mudeaters, creep, and folding over a few centimeters in the claystone of Sample 89 (Figs. 1g, 1h). The orientation of glauconite grains in such sectors is both parallel to bedding and transverse to bioturbation, indicating their diagenetic origin. Samples 89 and 89/1 contain mainly globular, anhedral, and fine-grained glauconite segregations, whereas the coarse-grained variety is subordinate.

It is worth mentioning that the irregular (often, clastic) shape of glauconite grains in present-day bioturbation sediments is related to their multiple reworking by fucoids (Geptner and Ivanovskaya, 1998). Such structures are lacking in the Virbalis section.

Green lamellae, which are subordinate in all samples, represent compositional analogues of globular glauconite and pseudomorphs of brown mica (biotite). The biotite to glauconite transition at the diagenetic stage has been studied using the latest methods and reported in several publications (Galliher, 1935; Ivanovskaya *et al.*, 1993, 2003; Kopeliovich, 1965; Murav'ev, 1962; Triplehorn, 1966; and others). For example, Ivanovskaya *et al.* (2003) investigated the dynamics of dioctahedral glauconite formation as a result of the structural rearrangement of trioctahedral biotite and discovered that biotite was transformed at the diagenetic stage with the utilization of the micaceous matrix in accordance with the solid phase mechanism. The development of platy and felted (microaggregate) texture within a single lamella indicates that the transformation is locally accompanied by the synthesis of a normal glauconite microaggregate. We also observed this process in separate green plates under a scanning electron microscope.

Diagenesis also promotes the replacement of vermicular remains and local sectors of brachiopod shells by glauconite (up to the point of complete pseudomorphism). Relative to the globular counterpart, the vermicular glauconite has a higher Fe concentration, indicating that organic matter is a favorable medium for glauconite formation.

Glauconite coatings on quartz grains are locally sealed by the regeneration quartz, suggesting their formation at the diagenetic stage. The interstitial glauconite can be generated by both diagenetic and catagenetic processes.

Deep Catagenetic Stage

Deep catagenetic transformations of terrigenous–clayey rocks of the Virbalis Formation are indicated by the development of conformable and incorporation boundaries between the quartz and feldspar grains, regeneration (sometimes, polyhedral) quartz cement, and typical clay mineral assemblage of dioctahedral micas (Fe-illites) and trioctahedral Fe^{2+}–Mg-chlorite.

The ductile deformation of glauconite grains under high *PT* conditions of deep catagenesis is differently manifested in various (or similar) rocks even within a single layer. For example, one can observe the development of convexo-concave surface of globules in some sectors and the formation of specific globular festoons and matrix (or splitting of grains) in other sectors (Figs. 2a–2f). This process prevails in the clay-poor sandy–silty layers and sectors. In the clay-rich rocks, the deformation is weaker and the globules are oblate.

As was mentioned above, globular glauconite deformation is typical of the Precambrian–Cambrian terrigenous rocks altered by deep catagenetic processes in northern and eastern Siberia, southern Urals, Podolsk area of the Dniester region, and Srednii Peninsula (Ivanovskaya, 1996; Ivanovskaya *et al.*, 1985, 1989, 1993, 2003). Intense deformations result in the loss of Fe, Mg, and Ca and gain of Al, i.e., recrystallization of glauconite (Ivanovskaya *et al.*, 1985).

Deep catagenetic transformations lead to not only the deformation of glauconite grains, but also their dissolution and replacement by clay minerals or quartz to a variable extent.

Based on the study of microtextural interrelations of glauconite grains and ambient terrigenous components, as well qualitative microprobe analyses using a scanning electron microscope equipped with Link-860, Geptner revealed that a reverse process (replacement of quartz by authigenic glauconite) could also take place during the deep catagenesis. Some glauconite grains have an authigenic glauconite coating often observed as a weakly crystallized (homogeneous) aggregate with poorly discernible individual flakes, suggesting their formation in the process of catagenesis. The glauconite shell related to diagenesis should develop a prominent flaky structure (similar to that of the groundmass of globular glauconite and mineralized vermicular remains) in the process of burial and catagenetic transformation.

The mechanism of authigenic glauconite formation in deep sequences remains a debatable issue. Like in the zone of diagenesis, the dissolution of quartz and formation of glauconite shell at the boundary with glauconite grains under conditions of deep catagenesis could involve microorganisms (Geptner and Ivanovskaya, 1998, 2000).

Dolomite, the youngest authigenic mineral, serves as interstitial and basal cement. It replaces both clastic and authigenic grains (quartz, feldspars, mica flakes, globular glauconite, and others). Its origin is probably related to compositional changes in formation waters during the Hercynian orogeny of the studied area (Vinogradov *et al.*, 2002). Impact of these events on the structural, crystallochemical, and isotope-geochemical

signature of glauconite is a subject for the future communication.

CONCLUSIONS

Glauconite is widespread in terrigenous–clayey rocks of the Lower Cambrian Virbalis Formation in western Lithuania.

In clay-rich horizontal-bedded sandstones, siltstones, and mudstones with the specific ichnostructure, glauconite formed without hiatuses and erosions at the stage of diagenetic transformation of sediments. In oblique-bedded sequences, glauconite grains underwent diagenetic transformations after short-term episodes of rock erosion.

The glauconite globules and matrix formed at the diagenetic stage. At the same time, glauconite replaced biotite flakes (up to the point of complete pseudomorphism), vermicular remains, and some sectors of brachiopod shells. The glauconite also corroded clastic quartz and feldspar grains.

Deep catagenetic transformation of rocks resulted in the deformation of glauconite grains and their replacement by illite–chlorite and/or quartz. The intensity of glauconite transformation was variable even within a single layer.

We suppose that the deep catagenesis promoted the formation of authigenic glauconite that replaces quartz and/or makes up a thin coating on some glauconite grains.

In the studied rocks, globular dioctahedral (2 : 1) layered silicates are represented by two mica phases (glauconite and subordinate illite). The two-phase composition of micaceous minerals can be observed at the microtextural level in rocks of different compositions and ages (Tsipurskii *et al.*, 1992). This specific feature is a consequence of formation constraints rather than transformations of one phase (glauconite) into another phase (illite). Micaceous phases with different Fe contents crystallize in nonequilibrium diagenetic conditions probably as result of the vital activity of bacteria.

ACKNOWLEDGMENTS

This work was carried out in the framework of fundamental studies sponsored by the Division of Earth Sciences, Russian Academy of Sciences (Program no. 6 “Problems of the Origin and Evolution of the Earth’s Biosphere”) and supported by the Russian Foundation for Basic Research (project nos. 02-05-64210, 02-05-64333).

REFERENCES

Brangulis, A., Murnieks, A., Nagle, A., and Friedrichsone, A., The Mid-Baltic Vendian and Cambrian Facies Section, in *Fatsii i stratigrafiya venda i kembriya zapada Vostochno-Evropeiskoi platformy* (The Vendian and Cambrian Facies and Stratigraphy in the Western Part of the East European Craton), Tallinn: Nauka, 1986, pp. 24–33.

Burst, J.F., Mineral Heterogeneity in “Glauconite” lamellae, *Am. Mineral.*, 1958, vol. 43, no. 5/6, pp. 481–497.

Clauer, N., Stille, P., Keppens, E., and O’Neil, J.R., Le mechanism de la glauconitisation: Apports de la geochimie isotopique d strontium, du neodyme et de l’oxygene de glauconies recentes, *C.R. Acad. Sci. Paris*, 1992, vol. 315, Ser. 2, no. 3, pp. 321–327.

Drits, V.A., Kameneva, M.Yu., Sakharov, B.A., Dainyak, L.G., Tsipurskii, S.I., Smolyar, B.B., Bukin, A.S., and Salyn, A.L., *Problemy opredeleniya real’noi struktury glaukonitov i rodstvennykh tonkodispersnykh fillosilikatov* (Problems of the Identification of the Real Structure of Glauconites and Associated Fine-Dispersed Phyllosilicates), Novosibirsk: Nauka, 1993.

Fenoshina, U.I., Glauconite from Lower Tortonian Rocks of the Lyuben Resort, in *Voprosy mineralogii osadochnykh obrazovanii* (Problems of the Mineralogy of Sedimentary Rocks), L’vov: Gos. Univ., 1961, pp. 226–282.

Formozova, L.N., *Glaukonitovye peski urochishcha Kyzyl-Sai* (Glauconitic Sands in the Kyzyl-Sai Area), Moscow: Akad. Nauk SSSR, 1949.

Galliher, E.W., Glauconite Genesis, *Bull. Geol. Soc. Am.*, 1935, vol. 46, pp. 1351–1366.

Geptner, A.R. and Ivanovskaya, T.A., Biochemogenic Genesis of the Glauconite–Nontronite Series Minerals in Present-Day Sediments of the Pacific Ocean, *Litol. Polezn. Iskop.*, 1998, no. 6, pp. 563–580 [*Lithol. Miner. Resour.,* 1998, vol. 33, no. 6, p. 503–517].

Geptner, A.R. and Ivanovskaya, T.A., Glauconite from the Lower Cretaceous Marine Rocks of England: A Concept of Biochemical Origin, *Litol. Polezn. Iskop.*, 2000, no. 5, pp. 487–499 [*Lithol. Miner. Resour.,* 2000, vol. 35, no. 5, pp. 434–444].

Geptner, A.R., Ivanovskaya, T.A., and Ushatinskaya, G.T., Problem of the Biochemogenic Origin of Layered Silicates of the Glauconite–Illite Composition, *Litol. Polezn. Iskop.*, 1994, no. 1, pp. 79–91.

Gorbunova, L.I., Glauconites in Jurassic and Lower Cretaceous Rocks of the Central Russian Platform, *Tr. IGN, Geol. Ser.*, 1950, vol. 114, no. 40, pp. 65–103.

Gorbunova, L.I., Glauconite from Lower Cretaceous Rocks in the Northeastern Caucasus, *Voprosy mineralogii osadochnykh obrazovanii* (Problems of the Mineralogy of Sedimentary Rocks), L’vov: Gos. Univ., 1961, pp. 92–121.

Hadding, A., *Glauconite and Glauconite Rocks. Pre-Quaternary Sedimentary Rocks of Sweden*, Zunds, 1932, pp. 1–175.

Hower, J., Some Factors Concerning the Nature and Origin of Glauconite, *Am. Mineral.*, 1961, vol. 46, no. 3/4, pp. 313–334.

Ivanovskaya, T.A., Glauconite–Illite Minerals in Upper Vendian–Lower Cambrian Boundary Deposits of Podolia, Dniester Region, *Litol. Polezn. Iskop.*, 1996, no. 6, pp. 509–521 [Lithol. Miner. Resour., 1996, vol. 31, no. 6, pp. 524–534].

Ivanovskaya, T.A., Tsipurskii, S.I., Cherkashin, V.I., and Yakhontova, L.K., Postsedimentary Alterations of Glauconite in Riphean Rocks of Southeastern Yakutia, *Izv. Akad. Nauk SSSR, Ser. Geol.*, 1985, no. 12, pp. 108–118.

Ivanovskaya, T.A., Tsipurskii, S.I., and Yakovleva, O.V., Mineralogy of Riphean and Vendian Globular Layered Silicates in Siberia and the Urals, *Litol. Polezn. Iskop.*, 1989, no. 3, pp. 83–99.

Ivanovskaya, T.A., Kats, A.G., Frolova, Z.B., Tsipurskii, S.I., and Yakovleva, O.V., Structure, Lithology, and Mineralogy of the Basal Lower Riphean in the Olenek High (Osorkhayata Formation), *Stratigr. Geol. Korrelyatsiya*, 1993, vol. 1, no. 4, pp. 84–92.

Ivanovskaya, T.A., Gor'kova, N.V., Karpova, G.V., Pokrovskaya, E.V., and Drits, V.A., Chloritization of Globular and Platy Silicates of the Glauconite Series in Terrigenous Rocks of the Upper Riphean Päräjarvi Formation (Srednii Peninsula), *Litol. Polezn. Iskop.*, 2003, no. 6, pp. 584–598 [*Lithol. Miner. Resour.* 2003, no. 6, pp. 495–508].

Jankauskas, T., *Cambrian Stratigraphy of Lithuania*, Vilnius, 2002.

Kohler, E.E. and Koster, H.M., Remarks on the Influence of Depositional Environment on Radiometric Dating, *Geol. Jahrbuch*, 1982, no. 52, pp. 101–111.

Kohler, E.E. and Koster, H.M., Zur Mineralogie, Kristallographie, und Geochemie Kretazischer Glauconite, *Clay Minerals*, 1976, vol. 11, pp. 273–302.

Kopeliovich, A.V., *Epigenez drevnikh tolshch yugo–zapada Russkoi platformy* (Epigenesis of Ancient Rock in the Southwestern Russian Platform), Tr. Geol. Inst. Akad. Nauk SSSR, 1965, no. 121.

Lazarenko, E.K., Problem of the Nomenclature and Classification of Glauconite, in *Voprosy mineralogii osadochnykh obrazovanii* (Problem of the Mineralogy of Sedimentary Rocks), L'vov: Gos. Univ., 1956, vols. 3–4, pp. 345–379.

Lipkina, M.I., Glauconitic Rocks on Volcanic Mounts in the Sea of Japan, *Litol. Polezn. Iskop.*, 1980, no. 4, pp. 44–54.

Lisitsina, N.A. and Butuzova, G.Yu., Problem of the Genesis of Oceanic Glauconites, *Litol. Polezn. Iskop.*, 1981, no. 5, pp. 91–97.

Lisitsina, N.A., Gradusov, B.P., and Butuzova, G.Yu., Glauconite in Sediments of the Transpacific Lithological Section, *Paleontologiya. Morskaya geologiya* (Paleontology. Marine Geology), Moscow: Nauka, 1976, pp. 166–176.

Logvinenko, N.V., Volkov, I.I., and Rozanov, A.G., Problem of the Genesis of Glauconite in Sediments of the Pacific Ocean, *Litol. Polezn. Iskop.,* 1975, no. 2, pp. 3–13.

Murav'ev, V.I., Epigenetic Transformations of Mesozoic Rocks in the Southeasterm Russian Platform, *Izv. Akad. Nauk SSSR, Ser. Geol.*, 1962, no. 6, pp. 34–47.

Murav'ev, V.I., *Mineral'nye paragenezy glaukonitovo–kremnistykh formatsii* (Mineral Assemblages of Glauconitic–Siliceous Formations), Moscow: Nauka, 1983.

Nikolaeva, I.V., *Mineraly gruppy glaukonita v osadochnykh formatsiyakh* (Minerals of the Glauconite Group in Sedimentary Rocks), Novosibirsk: Nauka, 1977.

Nikolaeva, I.V., Facies Zonality of the Chemical Composition of the Glauconite-Group Minerals and Factors of Their Control, *Mineralogiya i geokhimiya glaukonita* (Mineralogy and Geochemistry of Glauconite), Novosibirsk: Nauka, 1981, pp. 4–14.

Nikolaeva, I.V., *Ispol'zovanie glaukonita v geokhronologii (kalii–argonovaya sistema)* (The Application of Glauconite in Geochronology: Potassium–Argon System), Novosibirsk: Nauka, 1986.

Odin, G.S. and Matter, A., De Glauconarium Origine, *Sedimentology*, 1981, vol. 28, pp. 611–641.

Odin, G.S., *De Glauconiarum, Constitutione, Origine, Aetateque* Paris: Universite Pierre et Marie Curie, 1975.

Pirrus, E.A., The Vendian and Cambrian Lithogenesis in the Northern Baltic Region, *DSc. (Geol.–Mineral.) Dissertation*, Leningrad: Vses. Geol. Inst., 1989.

Shutov, V.D., Drits, V.A., Kats, M.Ya., and Sokolova, A.L., Model of the Genesis of Globular Glauconite in the Flysch Formation, *Litol. Polezn. Iskop.*, 1983, no. 1, pp. 23–40.

Shutov, V.D., Kats, M.Ya., Drits, V.A., Sokolova, A.L., and Kazakov, G.A., Crystallochemistry of Glauconite as an Indicator of Its Depositional Environment and Postsedimentary Transformation, in *Kristallokhimiya mineralov i geologicheskie problemy* (Crystal Chemistry of Minerals and Geological Problems), Moscow: Nauka, 1975, pp. 74–81.

Smolyar, B.B. and Drits, V.A., Dependence of Parameter *b* of the Elementary Cell of Dioctahedral Mica from Chemical Composition, *Mineral. Zh.*, 1988, vol. 10, no. 6, pp. 10–16.

Strakhov, N.M., *Osnovy teorii litogeneza* (Fundamentals of the Theory of Lithogenesis), Moscow: Nauka, 1960, vols. 1–2.

Triplehorn, D.M., Morphology, Internal Structure and Origin of Glauconite Lamellae, *Sedimentology*, 1966, vol. 6, no. 4, pp. 247–266.

Tsipurskii, S.I., Ivanovskaya, T.A., Sakharov, B.A., Zvyagina, B.B., and Drits, V.A., The Nature of the Coexistence of Glauconite, Fe-Illite and Illite in Globular Micaceous Rocks of Various Lithological Types and Ages, *Litol. Polezn. Iskop.*, 1992, no. 5, pp. 65–75.

Valeton, I. and Abdul-Razzak, A., Glauconite der Oberkeide Nordwestdeutschlands, *Mitt. Geol.-Paleontol. Univ. Hamburg*, 1975, no. 44, pp. 537–556.

Valeton, I., Abdul-Razzak, A., and Klussmann, D., Mineralogy and Geochemistry of Glauconite Lamellae from Cretaceous Sediments in Northwest Germany, *Geol. Jahrbuch*, 1982, vol. 52, pp. 5–87.

Vinogradov, V.I., Bujakaite, M.I., Murav'ev, V.I., Burzin, M.B., and Veis, A.F., Isotopic Evidence of the Paleozoic Stage of Epigenetic Transformation of Vendian Sediments of the Russian Platform, *Litol. Polezn. Iskop.*, 2000, no. 5, pp. 524–534 [*Lithol. Miner. Resour.,* 2000, no. 5, pp. 454–461].

Wilberg, H.G., Glaukonit Genese und Lithofazies im Cenoman von Dortmund (Westfalen), *Neues Jahrb. Geol. Paleontol. Monatsh.*, 1980, no. 1, pp. 52–64.